

Momentum Distributions of Photons from Positrons Annihilating in Alkali Halides

A. T. STEWART* AND N. K. POPE

Chalk River Laboratories, Atomic Energy of Canada Limited, Chalk River, Ontario, Canada

(Received August 2, 1960)

The angular correlation of photons from the two-gamma decay of positrons in all sodium halides and all alkali chlorides has been measured. The data yields the momentum distribution of the two gamma rays which is also the momentum distribution of the annihilating electron-positron pairs. It is seen that the positive ion has very little influence on the momentum distribution in comparison with the negative ion. These distributions in momentum are compared with the distributions calculated from various models of electron and positron wave functions in the crystal. For fluorides and chlorides the electron-positron wave-function products which yield fits to the experimental data resemble Hartree-Fock free-ion electron wave functions. Both the wave-function products and the free-ion wave functions yield density distributions which are similar to the electron densities obtained by x-ray measurements. This conclusion makes improbable a model of single-particle wave functions describing both the electrons and the positron tightly bound to the negative ion.

I. INTRODUCTION

IN the past few years some knowledge of the electron structure of matter has been obtained by studying the radiation from positrons annihilating in various materials. Several features of the radiation have been studied including the lifetime of the positron in the material, the fraction of positron annihilations which occur by various modes, and the momentum carried away from the system by the annihilation radiation. The last method has been used successfully to determine the momentum distributions of the annihilating electrons in metals,¹⁻¹² the fraction of annihilations which occur by different mechanisms in several amorphous solids and gases,^{1,5,7,9,10,13-15} and to detect and measure polarizations of positrons emitted in beta decay as well as the polarization of their annihilation radiation.¹⁶⁻²⁰ This paper presents experimental data on the angular correlation of photons from positron annihilation in two systematic series of alkali halides; all the sodium halides and all the alkali chlorides. From the angular distribution of photons we obtain their

momentum distribution as discussed in the following section. This momentum distribution of the annihilation photons is then compared with the momentum distribution calculated from several models based on free-ion wave functions. Because these results do not duplicate the extensive series of data presented by Millett and Castillo-Bahena,²¹ and because in the one alkali halide (NaCl) examined by both groups there appear to be slight discrepancies, it seems worth while to publish our data in some detail.²² Some other measurements of the angular correlation of photons from positrons annihilating in alkali chlorides have been made by Lang and DeBenedetti¹⁰ and one (LiF) by March and Stewart.²³

Ferrell²⁴ has discussed the annihilation process in alkali halides. He concludes that thermalized positrons in "an ionic crystal do not capture electrons because there is no room in the crystal for the resulting positronium atoms." He proposes a model for the annihilation process which considers both electrons and positrons in the tight binding approximation. Making approximate calculations on the basis of this model he obtained an angular correlation function of characteristic alkali halide (triangular) shape, the width of which is inversely proportional to the Goldschmidt negative-ion radius. Although this correlation is observed, the width criterion alone is not a definitive property of a model. We compare the fit of the measured momentum distributions of photons from positrons annihilating in alkali halides with momentum distributions calculated for five models of electron and positron wave functions. It is found that the measured momentum distributions are incompatible with the assumption that both electrons and positrons are described by tight-binding wave functions.

* Now at Dalhousie University, Halifax, Nova Scotia.

¹ S. DeBenedetti, C. E. Cowan, W. R. Konneker, and H. Primakoff, *Phys. Rev.* **77**, 205 (1950).

² H. Maier-Leibnitz, *Z. Naturforsch.* **6a**, 663 (1951).

³ J. DesCloiseau and G. Ambrosino, *Compt. rend.* **237**, 1069 (1953).

⁴ A. T. Stewart and R. E. Green, *Phys. Rev.* **98**, 232(A) (1955).

⁵ L. A. Page, M. Heinberg, J. Wallace, and T. Trout, *Phys. Rev.* **98**, 206 (1955).

⁶ R. E. Green and A. T. Stewart, *Phys. Rev.* **98**, 468 (1955).

⁷ A. T. Stewart, *Phys. Rev.* **99**, 594 (1955).

⁸ G. Lang, S. DeBenedetti, and R. Smoluchowski, *Phys. Rev.* **99**, 596 (1955).

⁹ L. A. Page and M. Heinberg, *Phys. Rev.* **102**, 1545 (1956).

¹⁰ L. G. Lang and S. DeBenedetti, *Phys. Rev.* **108**, 914 (1957).

¹¹ A. T. Stewart, *Can. J. Phys.* **35**, 168 (1957).

¹² L. G. Lang and N. C. Hien, *Phys. Rev.* **110**, 1062 (1958).

¹³ M. Heinberg and L. A. Page, *Phys. Rev.* **107**, 1589 (1957).

¹⁴ S. D. Warshaw, *Phys. Rev.* **108**, 713 (1957).

¹⁵ R. L. deZafra and W. T. Joyner, *Phys. Rev.* **112**, 19 (1958).

¹⁶ L. A. Page, *Phys. Rev.* **106**, 394 (1957).

¹⁷ L. A. Page and M. Heinberg, *Phys. Rev.* **106**, 1220 (1957).

¹⁸ S. S. Hanna and R. S. Preston, *Phys. Rev.* **106**, 1363 (1957).

¹⁹ S. S. Hanna and R. S. Preston, *Phys. Rev.* **109**, 716 (1958).

²⁰ L. A. Page, *Phys. Rev.* **109**, 2215 (1958).

²¹ W. E. Millett and R. Castillo-Bahena, *Phys. Rev.* **108**, 257 (1957).

²² Comments about discrepancies between data of various groups may be found in reference 23.

²³ R. H. March and A. T. Stewart, *Can. J. Phys.* **37**, 1076 (1959).

²⁴ R. A. Ferrell, *Revs. Modern Phys.* **28**, 308 (1956).

II. EXPERIMENTAL

Description of Experiment

The annihilation of positrons with electrons in matter takes place usually by the emission of two gamma rays which, to conserve momentum, are emitted at 180° to each other in the center-of-mass system. If the center of mass is in motion with respect to an observer the angle between the photon directions departs from 180° by an amount of the order of v/c where v is the velocity of the center of mass and c is the velocity of light. For the low velocities of interest here the departure of the angle between the photon directions from 180° is proportional to the component of momentum of the annihilating pair parallel to the bisector of the propagation directions. The experimental arrangement for measuring the angle between the photons is shown schematically in Fig. 1. The parallel slit geometry was used because it is easy to calibrate and the data obtained are simple to interpret. Radiation from the annihilation of positrons in the specimen was detected in two 2-in. \times 2-in. cylindrical NaI(Tl) crystals and 6292 photomultipliers mounted behind 0.050-in. \times 1.5-in. horizontal slits in lead shields. The rate of coincidences in the two detectors was measured as a function of the vertical displacement of the specimen from the mid-point between the counters. Automatic equipment moved the specimen at 5-minute intervals and recorded the counting rate. The pulse-height analyzers selected pulses corresponding to photons in the energy range from about 200 to 600 kev. The positron emitter used was Cu^{64} made by irradiating copper foils in the NRX reactor.

The active copper foil was mounted about $\frac{1}{2}$ in. above the alkali-halide specimen and was shielded from direct view of the detectors. The alkali-halide specimens were multicrystalline reagent-grade chemicals. This apparatus is little changed from that used for the work on metals.¹¹

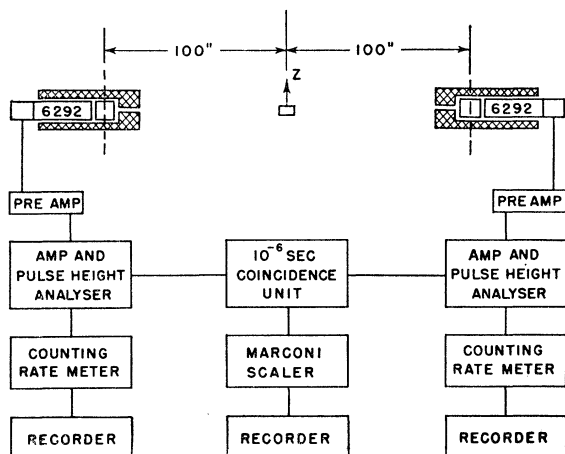


FIG. 1. Schematic diagram of the apparatus.

Results

The data obtained for both series of alkali halides are plotted in Fig. 2 where we have shown the coincidence counting rate as a function of the departure of the photon directions from 180° . The peak heights have been normalized to make them equal and the data have been corrected for the decay of the Cu^{64} source. For all specimens a peak count of 12 000 or greater was obtained.

None of the data have been corrected for instrument resolution effects. In the vertical direction the combined slit width and effective specimen thickness results in an approximately Gaussian-shaped resolution function of half-width about $0.7 \cdot 10^{-3}$ radian. This is much smaller than the width at half maximum of the effect being measured and so no correction is necessary. In the horizontal direction the finite length of the slits has negligible effect on the relative efficiency of counting annihilation events with various momenta, for the particular distribution of momentum obtained in this experiment.²⁵

III. MOMENTUM DISTRIBUTIONS

Reduction of Data

It has been shown¹¹ that for parallel-slit geometry the density of momentum vector points in momentum space, $\rho(p)$ and the momentum distribution, $N(p) = 4\pi p^2 \rho(p)$, may be obtained from the angular correlation data by the proportionality relations

$$N(p) \propto z dI/dz, \quad (1)$$

and

$$\rho(p) \propto (1/z) dI/dz, \quad (2)$$

where I is the coincidence counting rate as a function of z , the vertical displacement of the specimen from a line joining the detector slits. The centers of the observed distributions were taken to be $z=0$. The value of chord slope $(I_2 - I_1)/(z_2 - z_1)$ was used for the derivative dI/dz at $z = \frac{1}{2}(z_1 + z_2)$, where I_2 and I_1 are the counting rates at z_2 and z_1 , respectively. Momentum, p , and displacement, z , are related by $p = zmc/l$ where m is the electron mass and l is the distance from source to one detector. From these relations it is obvious that the slope of the angular correlation data, dI/dz , is proportional to momentum times momentum density, $p \rho(p)$. We have chosen to present (in Fig. 3) detailed results of the experiment in terms of the slopes of the measured angular correlation curves because this plot gives a more reliable impression of the accuracy of the experimental data than either the $\rho(p)$ and the $N(p)$ plots.²⁶

²⁵ It is easy to show that when the density distribution in momentum space, $\rho(p)$, is Gaussian the shape of the measured angular correlation curve is independent of slit length.

²⁶ In $\rho(p)$ and $N(p)$ plots, as can be seen in reference 11, the statistical errors shown for each point become very large and very small respectively as p decreases to zero.

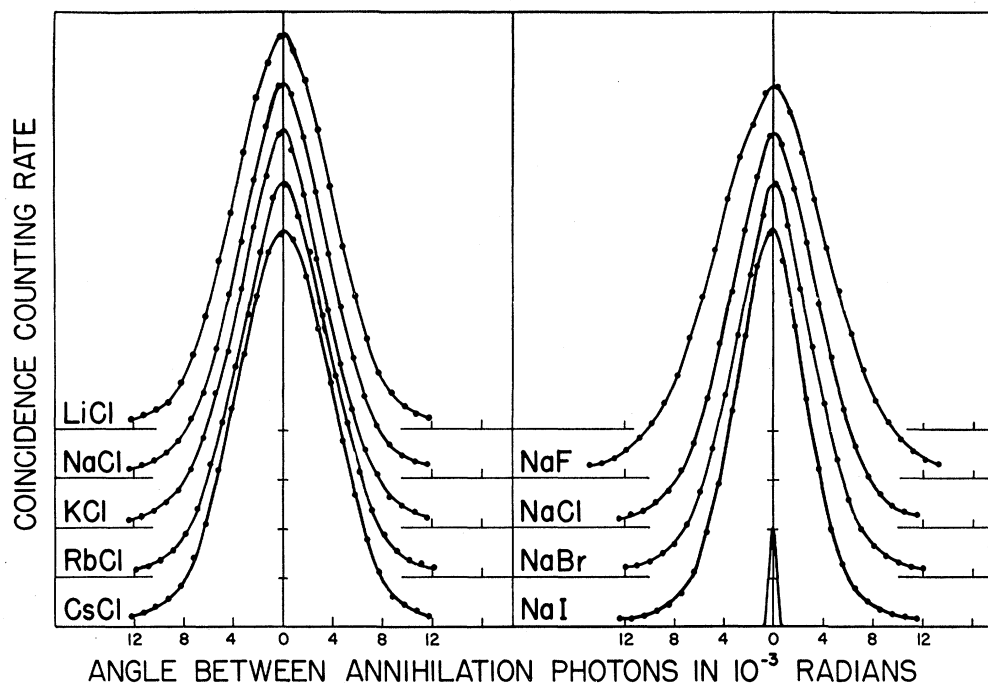


FIG. 2. Angular correlation data for all alkali chlorides and all sodium halides. The instrument resolution is also shown.

Qualitative Discussion

As early as 1950 DeBenedetti and co-workers¹ postulated that most annihilations of positrons in alkali halides should take place with the electrons of the negative ion. We present here a direct comparison of the experimental results for the two-gamma angular-correlation experiment for all alkali chlorides (Fig. 4) and all sodium halides (Fig. 5). It can be seen immediately that the halides are the dominating influence on the momentum of the annihilating pairs. Furthermore, a close inspection of Fig. 4 shows that the chlorides of sodium, potassium, and rubidium are very much alike while those of lithium and cesium are displaced somewhat to higher momentum. This result should possibly have been expected. In discussing ionic radii Pauling²⁷ has pointed out that in the case of lithium chloride the lithium ions are so small that the normal arrangement in the crystal is one in which a chlorine ion is in contact with twelve chlorine ions rather than six positive lithium ions. Thus the outer electrons of the chlorine ion are confined to a smaller volume and hence their momentum distributions are correspondingly extended. Cesium chloride differs from the other chlorides by having a body-centered cubic structure with each chlorine ion being in contact with eight positive ions instead of six as in the case of sodium chloride. Pauling²⁷ has explained the observed increase of the Cs-Cl distance over the sum of the radii of the cesium and chlorine ions, in terms of the extra repulsive forces,

²⁷ L. Pauling, *The Nature of the Chemical Bond* (Cornell University Press, Ithaca, New York, 1948), p. 355.

which arise from the increase in the number of positive ions around each chlorine ion. Thus, it is reasonable to suppose that, in this case too, there is a tendency for the outer electrons of the chlorine ions to be confined to a smaller volume.

IV. COMPARISON OF DATA WITH MODELS

Introduction

It has been shown^{24,28} that if the tight-binding approximation is valid for the electrons and if the positron can be represented by a Bloch wave function with wave vector zero, the characteristics of the annihilation of a positron with an electron in the crystal lattice are the same as for annihilation in any one crystal cell or probably in this case with the negative ion alone. Thus the probability amplitude $\chi_i(\mathbf{p})$, for the emission of two photons with total momentum, $\mathbf{p} = \hbar\mathbf{k}$, from the annihilation of a positron in a Bloch state Ψ_+ , with an electron in a state in which the space orbital localized on the same ion is Φ_i , is given by the Fourier transform of the wave-function product,

$$\chi_i(\mathbf{p}) = \frac{1}{h^3} \int e^{i\mathbf{k} \cdot \mathbf{r}} \Phi_i \Psi_+ d\mathbf{r}, \quad k = p/h. \quad (3)$$

From $\chi_i(\mathbf{p})$ we may form the momentum distribution, $N(p)$ by

$$N(p) = p^2 \sum_i \int |\chi_i(p)|^2 d\Omega, \quad (4)$$

²⁸ S. Berko and J. S. Plaskett, *Phys. Rev.* **112**, 1877 (1958).

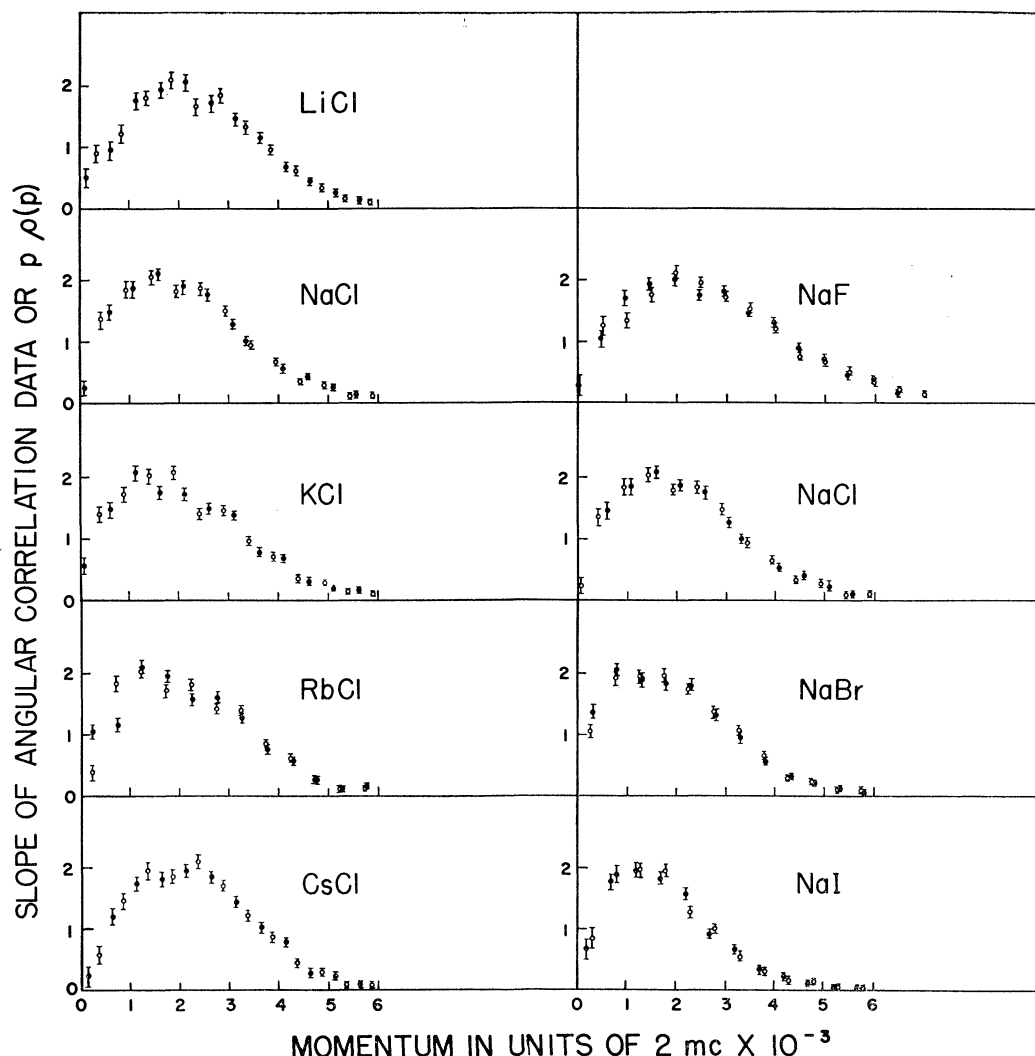


FIG. 3. Slopes of angular correlation data. These results are proportional to $p \rho(p)$.

where the integral is over all directions of the momentum \mathbf{p} and the summation is over all electrons. The terms in the summation are the squares of the momentum wave functions of the center of mass of the annihilating electron-positron pairs. In general these terms cannot be separated experimentally to obtain directly the momentum wave functions of the annihilating electron-positron pairs. For this reason we have calculated the momentum wave function for various models and present the results in the form $1/pN(p)$, or $p \rho(p)$, to compare with the experimental values of dI/dz .

In all models tried, hydrogen-like angular wave functions, i.e., normalized spherical harmonics, have been used for the angular dependent part of the atomic orbitals. Since the positron wave function is always assumed to be spherically symmetric, the angular dependence of the wave function product is the same as that for the electron.

By expanding $e^{i\mathbf{k} \cdot \mathbf{r}}$ in normalized spherical harmonics referred to some arbitrary fixed set of axes and using orthogonality properties and the addition theorem for the harmonics it is easily shown that

$$\chi_{nlm}(p, \theta, \phi) = h^{-3/2} 4\pi i^l \times \int_0^\infty j_l(kr) R_{nl}(r) R_+(r) r^2 dr \bar{Y}_m^l(\theta, \phi), \quad (5)$$

and

$$N_{nl}(p) = 4\pi 2 \sum_{-l}^l p^2 |\chi_{nlm}(p, \theta, \phi)|^2 = \frac{4(2l+1)}{\pi \hbar^3} p^2 \left| \int_0^\infty j_l(kr) R_{nl}(r) R_+(r) r^2 dr \right|^2, \quad (6)$$

where $\bar{Y}_m^l(\theta, \phi)$ is a normalized spherical harmonic,

TABLE I. Expressions for S_ν^{nl} .^a

$S_\nu^{1s} = \frac{2\gamma_\nu}{(\gamma_\nu^2 + k^2)^2}$
$S_\nu^{2p} = \frac{8\gamma_\nu}{(\gamma_\nu^2 + k^2)^3}$
$S_\nu^{2s} = \frac{2r_1\gamma_\nu}{(\gamma_\nu^2 + k^2)^2} - \frac{2(3\gamma_\nu^2 - k^2)}{(\gamma_\nu^2 + k^2)^3}$
$S_\nu^{3d} = \frac{48\gamma_\nu}{(\gamma_\nu^2 + k^2)^4}$
$S_\nu^{3p} = \frac{8\gamma_\nu r_1}{(\gamma_\nu^2 + k^2)^3} - \frac{8(5\gamma_\nu^2 - k^2)}{(\gamma_\nu^2 + k^2)^4}$
$S_\nu^{3s} = \frac{2r_1 r_2 \gamma_\nu}{(\gamma_\nu^2 + k^2)^2} - \frac{2(r_1 + r_2)(3\gamma_\nu^2 - k^2)}{(\gamma_\nu^2 + k^2)^3} + \frac{24\gamma_\nu(\gamma_\nu^2 - k^2)}{(\gamma_\nu^2 + k^2)^4}$

$$^a S_\nu^{nl} = k^{-l} \int_0^\infty r^{l+2} [(r_1 - r)(r_2 - r) \cdots] j_l(kr) \exp(-\gamma_\nu r) dr.$$

$R_{nl}(r)$, $R_+(r)$ are the radial wave functions for the electron and positrons, respectively, and j_l is a spherical Bessel function. The last equation gives the momentum distribution arising from annihilations with a complete shell of electrons.

In all models investigated we have started by using approximate free ion wave functions for the electrons. Löwdin²⁹ has proposed that Hartree or Hartree-Fock radial wave functions can be fitted by the analytic form:

$$R_{nl}^0(r) = r^l (r_1 - r)(r_2 - r) \cdots \sum_{\nu=1}^{n+1} A_\nu \exp(-\gamma_\nu r), \quad (7)$$

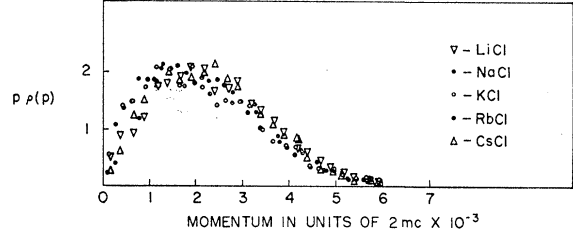
where for each n, l , the disposable constants are the r_i ,

 TABLE II. Electron wave function parameters for fluoride and chloride ions.^a

F ⁻								
1s			2s			2p		
ν	1	2	1	2	3	1	2	3
A_ν	48.847	2.257	20.254	24.328	2.8784	10.5080	7.5800	0.53324
γ_ν	8.9004	5.4315	6.6954	3.4685	1.8460	5.6022	2.5525	1.0724
$r_1 = 0.24409$								
Cl ⁻								
1s			2s			2p		
ν	1	2	1	2	3	1	2	3
A_ν	49.235	87.03	51.335	156.77	97.310	22.594	77.535	52.344
γ_ν	14.329	18.381	5.3545	7.6112	12.6846	4.7395	6.8437	11.9160
$r_1 = 0.12480$								
3s						3p		
ν	1	2	3	4	1	2	3	4
A_ν	1.6874	27.507	80.475	57.540	0.13472	3.2595	22.402	41.722
γ_ν	1.7189	3.063	5.4822	11.1332	0.9958	1.9059	3.4929	7.3684
$r_1 = 0.1216$			$r_2 = 0.55499$		$r_1 = 0.53153$			

^a The values for F⁻ were obtained by Pope and Kennedy (reference 31) and for Cl⁻ by Löwdin and Appel (reference 29). All the parameters are expressed in atomic units.

²⁹ P. O. Löwdin and K. Appel, Phys. Rev. **103**, 1746 (1956).


 FIG. 4. Comparison of $p \rho(p)$ results for all alkali chlorides.

A_ν , and γ_ν and there are $(n-l-1)$ nodes located at the positions $r=r_i$.

The momentum distribution for the electrons belonging to a given shell, $N_{nl}^e(p)$, can be calculated by substituting

$$R_{nl}(r) = R_{nl}^0(r), \quad R_+(r) = 1, \quad (8)$$

in Eq. (6) for $N_{nl}(p)$. The results can be written in the form

$$N_{nl}^e(p) = \frac{4(2l+1)}{\pi \hbar} k^{2l+2} \left| \sum_\nu A_\nu S_\nu^{nl} \right|^2,$$

where the S_ν^{nl} are given in Table I. Löwdin has fitted the Hartree radial functions with exchange for all

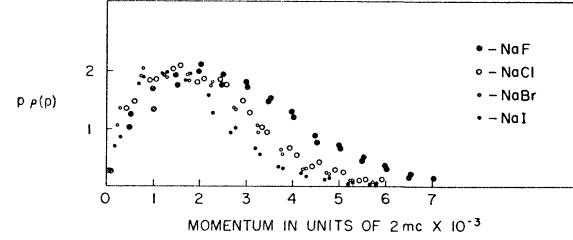

 FIG. 5. Comparison of $p \rho(p)$ results for all sodium halides.

TABLE III. Model radial wave functions. The table shows the forms of the positron radial wave functions, $R_+(r)$, and the electron radial wave functions, $R_{nl}(r)$, which have been used to calculate, $N_{nl}(p)$, the center-of-mass momentum distribution of the annihilating pairs. Also shown are values of the parameters which make $N_{nl}(p)/p$ a best fit to the slope of the measured angular correlation function.

Model	$R_+(r)$	$R_{nl}(r)$	Negative ion	Best parameters ^a	Fit
A	$e^{-\alpha r}$	$R_{nl}^0(r)^b$	Fl ⁻	$\alpha = -0.2$	poor
			Cl ⁻	$\alpha = -0.1$	poor
B	$re^{-\alpha r}$	$R_{nl}^0(r)$	Fl ⁻	$\alpha = 0$	poor
			Cl ⁻	$\alpha = 0.4$	fair
C	$\exp[-\beta(b-r)^2]$	$R_{nl}^0(r)$	Fl ⁻	$b \approx 6.0$	fair ^c
				$\beta \approx 0.2$	
			Cl ⁻	$b \approx 4.5$	fair ^c
				$\beta \approx 0.2$	
D	1	$N_{nl}e^{-\alpha_{nl}r}R_{nl}^0(r)^d$	Fl ⁻	$\alpha_{2s} = -0.6$	fair
				$\alpha_{2p} = 0$	
			Cl ⁻	$\alpha_{3s} = -0.3$	fair
				$\alpha_{3p} = 0$	
E	1	$e^{-\alpha_{nl}r}R_{nl}^0(r)^e$	Fl ⁻	$\alpha_{2s} = -0.1$	good
				$\alpha_{2p} = 0.3^f$	good
			Cl ⁻	$\alpha_{3s} = 0.1^g$	good
				$\alpha_{3p} = 2.4$	fair
		$e^{-\alpha_{nl}r}r^n$	Br ⁻	$\alpha_{4s} = 2.5$	fair
			I ⁻	$\alpha_{5s} = 2.5$	fair

^a Atomic units are used (reference 30).

^b Löwdin type radial functions.

^c Fit not sensitive to values of the parameters.

^d N_{nl} is a normalizing constant.

^e The annihilating electrons are assumed to be in $2s$ orbitals for F⁻ and $3s$ orbitals for Cl⁻.

^f LiCl and CsCl.

^g NaCl, KCl, and RbCl.

electrons of the chloride ion, Cl⁻. The parameters he obtained²⁹ are given in Table II.³⁰ The corresponding parameters³¹ for the fluoride ion, F⁻, are also shown in the table. It can be shown that only the outer electrons of the negative ions make a significant contribution to the momentum distribution in the range of measurement. For the bromide and iodide ions, for which Hartree calculations are not available we have used a Slater-type radial wave function, of the form $r^n \exp(-\gamma r)$, for the outer electrons only.

The models investigated differed in the forms chosen for the electron radial wave function, $R_{nl}(r)$, and the positron radial wave function $R_+(r)$. Table III gives in summary form the electron and positron radial functions used in each model. The expressions for $R_{nl}(r)$ and $R_+(r)$ were substituted in Eq. (6) for the momentum distribution $N_{nl}(p)$ and parameters in $R_{nl}(r)$ and $R_+(r)$ were adapted so that values of $N_{nl}(p)/p$ calculated from Eq. (6) gave best agreement with the measured values of dI/dz . The best values of the parameters obtained for five different models and comments on the quality of the fit are also given in Table III. Figures 6, 7, and 8 show the best fits obtained

for these five models. We discuss first the fits to the alkali chlorides.

Tight-Binding Positron Wave Function

Model A uses a bound positron with a radial wave function $\exp(-\alpha r)$ and free ion electrons. The momentum distribution for this model has the same form as for the free ion electrons [Eq. (9) and Table I] with the γ_v replaced by $\gamma_v + \alpha$. To obtain any reasonable fit α was found to be negative. This of course invalidates the assumption of a positron tightly bound to a negative ion, the electrons of which are described by free-ion wave functions.

Model B uses $re^{-\alpha r}$ for the positron wave function and free-ion electron wave functions. The position of the maximum of the momentum distribution for this model can be made to fit the observed results. When this is done however, the width of the calculated momentum distribution is too narrow. While positive values of α are found for the chloride ion, the absolute magnitudes of these values are so small that the positron wave function is not confined to its chloride ion and so the assumption of a positron which is tightly bound to the negative ion, is invalidated just as for model A.

Model C uses a positron radial wave function of Gaussian form with a maximum at $r=b$, and free-ion electron wave functions. Momentum distributions for this model were calculated numerically. For each alkali chloride a nonlinear least squares fit to the data was performed on the Chalk River Datatron to obtain best values of β , b and a normalizing constant. It should be noted that if b is taken to be slightly less than the Goldschmidt radius of the negative ion and β is large, this model is the same type as that proposed by Ferrell. Any reasonable fit, however, required a very broad Gaussian with a maximum well out beyond the ion radius.³² Only that small part of the positron wave function which overlaps the electron wave functions of the chloride ion at the origin is determined by the

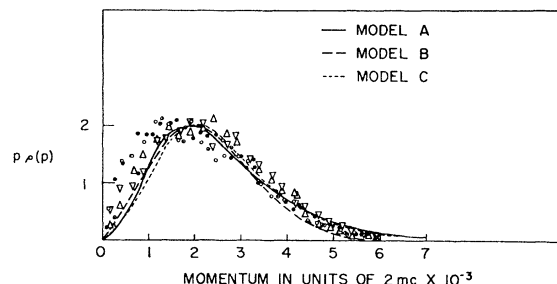
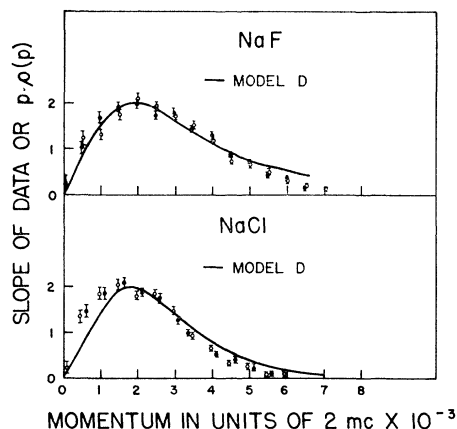


FIG. 6. Best fits to alkali chloride data obtained with models A, B, and C. The legend for the points is given in Fig. 4.

³⁰ All parameters occurring in electron or positron wave functions are expressed in atomic units. See D. R. Hartree, *The Calculation of Atomic Structures* (John Wiley & Sons, Inc., New York, 1957), pp. 5-6.

³¹ These parameters were obtained by one of us (N.K.P.) and Dr. J. M. Kennedy by nonlinear least squares fitting to Hartree wave functions with exchange.

³² The values of β and b which we quoted in Bull. Am. Phys. Soc. 4, 217 (1959) and are said to give a good fit are incorrect. As stated at the meeting, they arose from a breakdown in accuracy in a Gaussian-integration subroutine which resulted in values for β and b in remarkable agreement with preconceived ideas.

FIG. 7. Best fits to sodium halide data with model *D*.

data. The remainder has no significance. This model, like the previous two, invalidates the assumption of a positron tightly bound to the negative ions, the electrons of which are described by free-ion wave functions.

From a consideration of the above models we may conclude that to obtain a momentum distribution in the observed momentum range we need a space wave function product that is approximately the same size as the free-ion electron wave functions. We conclude that unless the electrons of the negative ion expand considerably when placed in the fields of a crystal lattice the positron cannot be considered localized on a single negative ion.

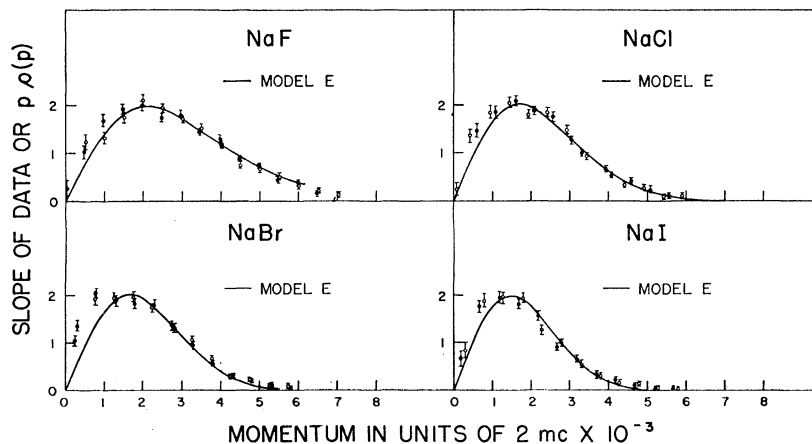
Plane-Wave Positron Wave Function

In view of the failure of the tight-binding approximation for the positron wave function we have considered the other extreme, viz., a free positron represented by a plane wave. For the lowest energy positron wave function we have put $\Psi_+ = 1$ and have investigated the changes which must be made to the free-ion electron wave functions to give a satisfactory fit. In model *D*

we obtained a fair fit (Fig. 7) by dilating the *s* and *p* wave functions differently (see Table III). It is tempting to assume that the positron wave function is approximately constant in the region of the 3*s* and 3*p* electrons and to interpret the wave function changes as the effect of the crystalline fields on the outer electrons. In general, the calculated distributions are too small for small *p*. The fit could be improved by extending the tails of the radial electron orbitals, thus suggesting a partial breakdown of the tight-binding approximation for the electrons. Electron-positron correlation effects may also play a part in determining the shape of the momentum distribution for small *p*.

Model E (phenomenological). In computing the fits for model *D* we observed that a good fit (Fig. 8) to the momentum distribution could be obtained with a model which assumed a plane wave positron and annihilations by *s*-type electrons only. We have not been able to find a physical interpretation for this model. On the one hand, there seems to be no physical reason why there should be a selection rule which prevents annihilation with *p* electrons and lifetime results make such an interpretation very unlikely. On the other hand, we cannot justify the assumption that the eight outer-shell electrons are all in *s*-type orbitals. The reason why model *E* tends to give a better fit than model *D* can be seen from Eq. (6). For small *p*, $N_{nl}(p)/p$ is proportional to *p* for *s*-type electron orbitals and to p^3 for *p*-type orbitals. In all the models, the calculated $N_{nl}(p)/p$ tends to be too small for small values of *p* and hence it is easier to fit the results using *s*-type orbitals for the electrons than it is using *p*-type orbitals.

Similar results were obtained in fitting the data from positrons annihilating in NaF and LiF²³ and the parameters obtained are shown in Table III. The only attempt to fit the NaBr and NaI data, because of the lack of free-ion wave functions, was made with model *E*. As for fluorine and chlorine a reasonable fit was obtained using only the *s*-type orbitals. The parameters are shown in the table and the fits in Fig. 8.

FIG. 8. Best fits to sodium halide data with model *E*.

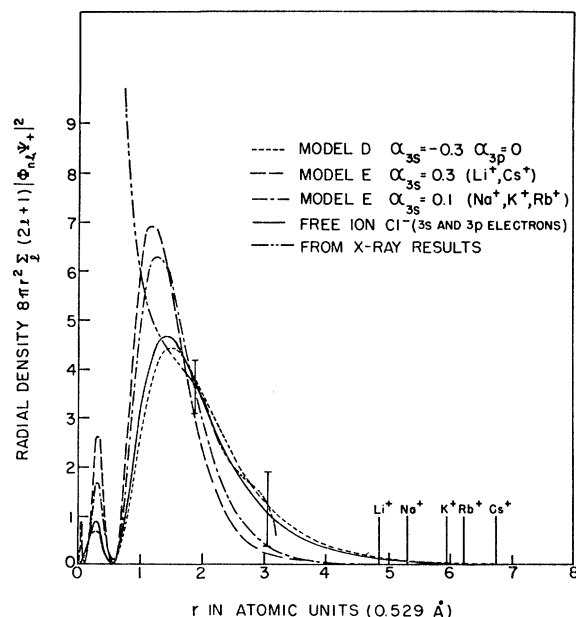


FIG. 9. Radial distributions from space wave functions for models *D* and *E* fitted to chloride data. In model *E* it is arbitrarily assumed that there are eight electrons in a 3s orbital. The electron radial distribution from x-ray measurements and from Hartree-Fock free-ion wave functions are also shown. The error bars refer to errors in the x-ray measurements (see reference 35). The positions of the nearest alkali ions are shown by vertical lines at the appropriate radial distances.

In Fig. 9 we have plotted for the chloride ion the radial distribution of the center of mass of electron-positron pairs from the wave functions which give fits for models *D* and *E*. For the phenomenological model *E*, the radial density has been normalized to eight electrons. For comparison we also show the radial distribution of outer shell (3s and 3p) electrons for the Hartree-Fock free ion. It is seen that models which fit the measured momentum distribution have a radial distribution of electrons similar to the radial distribution of the outer shell of the free ion. In the same figure is also shown an average radial distribution of electrons in the outer shell of the chloride ion in sodium chloride as determined from x-ray measurements of the electron density in the $(x,y,0)$ plane.³³⁻³⁵ Outside the 2s-2p shell this averaged measured density agrees with the calculated free ion density thus suggesting that the use of tight-binding wave functions for the electrons is a good approximation. Within the experi-

³³ H. Witte and E. Wölfel, Z. physik. Chem. 3, 296 (1955).

³⁴ H. Witte and E. Wölfel, Revs. Modern Phys. 30, 51 (1958).

³⁵ If values of the electron density, measured by Witte and Wölfel at points $(x,y,0)$ are plotted as a function of r , the distance from the center of the chloride ion, one does not obtain a smooth curve due to deviations of the electron density from spherical symmetry and to experimental error. The average radial distribution plotted in Fig. 9 (and similarly in Fig. 10) is a smooth curve through such points. The error bars represent an estimate of the experimental error on the individual points at the corresponding value of r .

mental uncertainties, the x-ray results agree with the results for models *D* and *E* and thus lend support to the hypothesis that the effective positron wave function is relatively constant over the region of space occupied by the outer shell electrons of the negative ion.

Figure 10 shows the same information for the fluoride ion and the comparison with x-ray results is taken from density measurements in the $(x,y,0)$ and (x,x,z) planes of LiF.³⁴⁻³⁶ The agreement between the different radial distributions is even better for this ion.

V. CONCLUSIONS

Angular distributions of photons from electron-positron annihilation in alkali halides have been measured. They show that the negative ion determines the momentum distribution of the annihilation gamma rays, the effect of changing the positive ion being hardly observable.

The data have been fitted with several models of electron and positron wave functions. The momentum distributions of the center of mass of the annihilating electron-positron pairs are comparable with the momentum distributions of the outer electrons calculated from Hartree-Fock, free-ion wave functions and are compatible with electron densities calculated from x-ray measurements. This leads to the conclusion that if the positron is to be represented by a single-particle

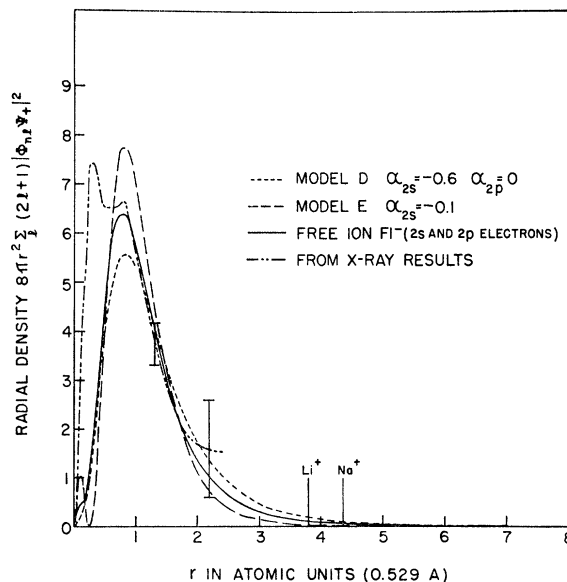


FIG. 10. Radial distributions from space wave functions for models *D* and *E* fitted to fluoride data. In model *E* it is arbitrarily assumed that there are eight electrons in a 2s orbital. The electron radial distributions from x-ray measurements and from Hartree-Fock free-ion wave functions are also shown. The error bars refer to errors in the x-ray measurements (see reference 35). The positions of the nearest alkali ions are shown by vertical lines at the appropriate radial distances.

³⁶ J. Krug, H. Witte and E. Wölfel, Z. physik. Chem. 4, 36 (1955).

wave function, it must not be considered as localized on any one negative ion. It is clear that to interpret the data uniquely simple models such as we have used³⁷ are not adequate but that accurate positron and electron wave functions are required.

³⁷ Another form is given in reference 21.

ACKNOWLEDGMENTS

It is a pleasure to thank Dr. Kennedy and the Datatron staff for help in computations, Mr. E. Glaser for considerable technical assistance, and to acknowledge the contributions colleagues have made in discussions.

Momentum Distribution of an Interacting Electron Gas*

E. DANIEL† AND S. H. VOSKO††

Department of Physics, University of California, La Jolla, California

(Received August 10, 1960)

The momentum distribution of an interacting electron gas at zero temperature is studied in the high-density region. Numerical computations are made for the graphs corresponding to the excitation of pairs, which are known to be equivalent to the random phase approximation of Bohm and Pines. Exchange graphs are discussed. The numerical results, extrapolated to actual electronic densities in metals, show that a large discontinuity in the momentum distribution still remains at the Fermi level.

1. INTRODUCTION

IN a noninteracting Fermi gas at zero temperature, the occupation probability of the individual particle energy levels is one for levels below the Fermi energy and zero for energies above the Fermi level. It is of interest to know to what extent the Fermi surface remains well defined in a real electron gas when the interaction between the particles is taken into account. Recently, Migdal¹ has shown that the characteristic discontinuity in the momentum distribution may still exist. In this paper, the momentum distribution is studied by perturbation theory. Since a discontinuity exists in zeroth order of the interaction, it is clear that it will persist. However, since the convergence of the expansion is questionable, this does not prove that the true ground state of the system will have such a discontinuity. The purpose of this paper is to estimate the magnitude of the discontinuity by a perturbation expansion, assuming that such an expansion has some validity.

Experimentally, the sharpness of the Fermi surface is strongly suggested by the de Haas-van Alphen effect, cyclotron resonance in metals and the existence of long-range interactions in metals and alloys through oscillating densities of the conduction electrons.²

It is clear that the Fermi surface is the more sharply defined the higher the electronic density. The reason

for this is that the average kinetic energy of the electrons increases as the square of their inverse average spacing, while their Coulomb energy increases only as the inverse of this spacing. As we consider the Coulomb interaction as a perturbation, we are justified in starting from a high-density case. Our calculation follows the same lines as Gell-Mann and Brueckner's calculation of the correlation energy of an electron gas.³

2. THE FICTIVE INTERACTION

We consider an electron gas in a very large volume Ω . Let k_F be the radius of the Fermi sphere for the noninteracting gas. Without Coulomb interactions, the normalized wave function for an electron with momentum $\mathbf{p}k_F$ and spin $s = \pm \frac{1}{2}$ would be⁴

$$\psi_{\mathbf{p},s} = (1/\Omega^{\frac{1}{2}}) \chi_s e^{i(\mathbf{p} \cdot \mathbf{r}) k_F}.$$

χ_s is the spin wave function and \mathbf{r} gives the spatial coordinates of the electron.

The density of states in the \mathbf{p} vector space is $\Omega k_F^3/8\pi^3$ for each direction of spin. At zero temperature, all the states with $p < 1$ would be occupied, and all the states with $p > 1$ would be empty. Using the second quantization formalism, we define this configuration as the vacuum for the interacting gas. We introduce the following creation and annihilation operators:

$a_{\mathbf{p},s}^*$, which creates an electron with momentum $\mathbf{p}k_F$ and spin s if $p > 1$ (it destroys a hole with momentum $-\mathbf{p}k_F$ and spin $-s$ if $p < 1$); and $a_{\mathbf{p},s}$, which annihilates an electron with momentum $\mathbf{p}k_F$ and spin s if $p > 1$ (it creates a hole with momentum $-\mathbf{p}k_F$ and spin $-s$ if $p < 1$).

³ M. Gell-Mann and K. A. Brueckner, Phys. Rev. **106**, 364 (1957).

⁴ The reduced Planck constant \hbar and the electron mass are set equal to one throughout this paper.

* This work was supported in part by the Office of Naval Research.

† Now at the Institute of Physics, Strasbourg, France.

†† Now at McMaster University, Hamilton, Ontario, Canada.

¹ A. B. Migdal, J. Exptl. Theoret. Phys. (U.S.S.R.) **32**, 399 (1957) [translation: Soviet Phys.—JETP **5**, 333 (1957)].

² M. A. Ruderman and C. Kittel, Phys. Rev. **96**, 99 (1954); A. Blandin, E. Daniel, and J. Friedel, Phil. Mag. **4**, 180 (1959); J. S. Langer and S. H. Vosko, J. Phys. Chem. Solids **12**, 196 (1959); W. Kohn and S. H. Vosko, Phys. Rev. **119**, 912 (1960).